

Strong Anderson localization in cold atom quantum quenches

T. Micklitz¹, C. A. Müller², and A. Altland³

¹*Centro Brasileiro de Pesquisas Físicas, Rua Xavier Sigaud 150, 22290-180, Rio de Janeiro, Brazil*

²*Fachbereich Physik, Universität Konstanz, 78457 Konstanz, Germany*

³*Institut für Theoretische Physik, Universität zu Köln, Zùlpicher Str. 77, 50937 Cologne, Germany*

(Dated: September 29, 2018)

Signatures of Anderson localization in the momentum distribution of a cold atom cloud after a quantum quench are studied. We consider a quasi one-dimensional cloud initially prepared in a well defined momentum state, and expanding for some time in a disorder speckle potential. Quantum interference generates a peak in the forward scattering amplitude which, unlike the common weak localization backscattering peak, is a signature of *strong* Anderson localization. We present a non-perturbative, and fully time resolved description of the phenomenon, covering the entire diffusion-to-localization crossover. Our results should be observable by present day experiments.

PACS numbers: 71.15.Rn, 42.25.Dd, 03.75.-b, 05.60.Gg

After several decades of research there remains a stark imbalance between a huge body of theory and scarcely any controlled experimental observation of Anderson localization in generic disordered systems [1]. Here ‘controlled’ means the option to link experimental signatures directly to underlying quantum interference processes via a tuneable parameter. Ultra-cold atoms are likely our best bet to improve upon this situation, and experiments based on a quench protocol appear to be particularly promising. Within the quench paradigm, ‘time’ plays the role of a control parameter, and Anderson localization would be monitored in the slow genesis of an observable strongly affected by disorder generated quantum interference. A specific proposal going in this direction has recently been made [2, 3] and realized [4, 5]. These experiments expose a cloud of cold atoms with initially well defined momentum, \mathbf{k}_i , to a laser speckle disorder potential. Suspended against gravity by magnetic levitation, the cloud propagates in the disorder potential for some time, t , after which all potentials are turned off and the atomic momentum distribution $\rho(\mathbf{k}_f, t)$ is determined by time of flight measurement.

For this setup, theory [3] predicts the presence of a forward scattering peak ($\mathbf{k}_f \simeq \mathbf{k}_i$), besides the familiar weak localization backscattering ($\mathbf{k}_f \simeq -\mathbf{k}_i$) peak often observed in such types of experiment. The remarkable difference between the two structures is that the forward peak is a manifestation of *strong* Anderson localization, i.e. a non-perturbative accumulation of quantum coherence processes. First indications to the emergence of a forward peak have been extracted from an insightful combination of perturbation and scaling theory in Ref. [3]. However, the full profile of the signal, its height, width, and temporal development, can only be addressed in terms of the non-perturbative methods tailored to the description of strong localization phenomena [6, 7]. At any rate, an observation of the peak formation — which arguably is in reach of present experimentation — and its successful comparison to time-resolved analytic results

would provide us with an exceptionally strong testbed for our understanding of strong localization phenomena.

In this paper, we present a fully analytic theory of the forward scattering peak in the quantum quench protocol. Particular attention is paid to the genesis of the peak at the time scale characteristic for the buildup of strong localization phenomena, an analysis made possible thanks to recent progress [8]. Our theory also describes the structure of the fully developed peak in momentum space, i.e. its height relative to the isotropic background, its width, and its dependence on the experimentally unavoidable initial momentum spread.

Below we consider a situation where time reversal (T) invariance is broken by a weak synthetic gauge field. In this case, the diffusion modes relevant to the formation of the backscattering peak (‘Cooperon modes’ in the parlour of the field) are frozen out, and the signatures of localization reside entirely in the forward peak. While the absence of Cooperon modes technically simplifies our analysis, strong localization is only weakly affected — e.g., the localization length doubles compared to the T invariant case — and the features of the forward peak are not expected to be modified in essential ways.

Model and effective theory:—We consider a cloud of non-interacting atoms confined to a quasi one-dimensional geometry of extensions $L_{y,z} \ll L_x$, and described by the Hamiltonian $\hat{H}_0 = (\hat{\mathbf{p}} - \mathbf{a})^2/2m$, where \mathbf{a} is a weak T-breaking synthetic gauge field [9, 10]. Assume the cloud to be initially prepared in a momentum eigenstate $|\mathbf{k}_i\rangle$; residual effects due to momentum spread will be discussed below. At time $t = 0$ we switch on a random potential, $\hat{H}_0 \rightarrow \hat{H} \equiv \hat{H}_0 + V(\hat{\mathbf{x}})$. Assuming V to represent a short range laser speckle, we model it as Gaussian white noise, $V(\mathbf{x})V(\mathbf{x}') = \frac{1}{2\pi\nu\tau}\delta(\mathbf{x} - \mathbf{x}')$, where ν is the density of states per volume, τ is the elastic scattering time, and \hbar has been set to unity.

The observable of interest is the time dependent con-

figuration averaged fidelity

$$\mathcal{C}_{\mathbf{k}_i, \mathbf{k}_f}(t) = \overline{|\langle \mathbf{k}_f | e^{-i\hat{H}t} | \mathbf{k}_i \rangle|^2}, \quad (1)$$

between initial and final state, which is directly measurable by time of flight absorption measurement. At times larger than the mean free time, the response function \mathcal{C} splits into a sum of two pieces,

$$\mathcal{C}_{\mathbf{k}_i, \mathbf{k}_f} \stackrel{t \geq \tau}{=} \mathcal{N} f_{\mathbf{k}_i} f_{\mathbf{k}_f} [\mathcal{C}_0 + \mathcal{C}_1(\mathbf{q})], \quad (2)$$

where \mathcal{C}_0 and \mathcal{C}_1 are the isotropic background and the momentum dependent contribution to the correlation function, resp., where $\mathbf{q} = \mathbf{k}_i - \mathbf{k}_f$ is the momentum difference, and the weight function $f_{\mathbf{k}} = [1 + (2\tau(\frac{k^2}{2m} - E))^2]^{-1}$ restricts initial and final momenta to a disorder-broadened shell of energy, E , and \mathcal{N} guarantees the normalization $\sum_{\mathbf{k}'} \mathcal{C}_{\mathbf{k}\mathbf{k}'}(t) = 1$.

Classical kinetic theory predicts that at time scales larger than the elastic scattering time, τ , the momentum distribution will diffusively relax to an isotropic configuration with $\mathcal{C}_1 = 0$ [11]. Quantum coherence introduces the Heisenberg time $t_H = 1/\Delta_\xi$, where Δ_ξ is the single particle level spacing of a ‘localization volume’. In our quasi one-dimensional setup, $\Delta_\xi = (2\pi\nu S\xi)^{-1}$, where $S = L_y L_z$ is the cross section of the system, and $\xi \gg L_{y,z}$ the longitudinal localization length due to disorder. The latter can be implicitly defined by the equality $\Delta_\xi = D/\xi^2$ to the inverse of the diffusion time through a localization volume as $\xi = 2\pi\nu S D$, where D is the three-dimensional diffusion constant on the energy shell. We assume the system to be strongly localizing in the sense $\xi \ll L_x$, at negligibly weak finite size corrections in ξ/L_x . In the following we will construct a microscopic theory of the appearance of this scale and its influence on the evolution of the forward peak.

We start out by Fourier transforming the correlation function to frequency space, $\mathcal{C}(t) = \int \frac{d\eta}{2\pi} \mathcal{C}(\eta) e^{-2it\eta}$, where $\eta^+ = \eta + i0$. The function $\mathcal{C}(\eta)$ then assumes the standard response form of a product of two single particle Green functions, which is to be averaged over disorder. Expressions of this type are tailored to an analysis in terms of the supersymmetric nonlinear σ -model, and a straightforward application of the formalism of Ref. [6] yields our momentum correlation functions as

$$\mathcal{C}_0(\eta) = \langle \text{tr}(\mathcal{P}_{++} Q(0) \mathcal{P}_{--} Q(0)) \rangle_{S_0}, \quad (3)$$

$$\mathcal{C}_1(\mathbf{q}, \eta) = \delta_{0, \mathbf{q}^\perp} \langle \text{tr}(\mathcal{P}_{-+} Q(\mathbf{q}) \mathcal{P}_{+-} Q(-\mathbf{q})) \rangle_{S_0}. \quad (4)$$

Here $Q = \{Q_{ss'}^{\alpha\alpha'}\}$ is a 4×4 supermatrix, that obeys the nonlinear constraint $Q^2 = \mathbb{1}$. Its diagonal 2×2 upper-left and lower-right matrix blocks Q^{bb} and Q^{ff} , resp., contain complex numbers, while the off-diagonal blocks $Q^{\text{bf,fb}}$ contain Grassmann variables. The subscript indices $Q_{s,s'}$, $s, s' = \pm$ discriminate between ‘retarded’ and ‘advanced’ components of the matrix field, and the matrices $\mathcal{P}_{ss'}$ project on the s, s' advanced/retarded block

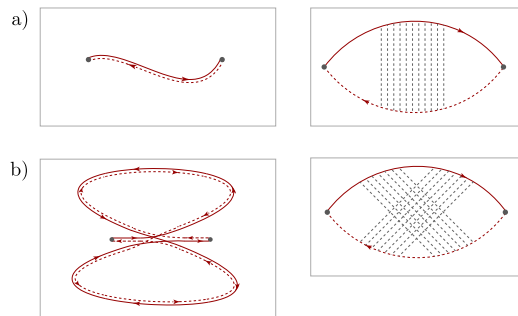


FIG. 1: Leading, a), and subleading, b), contributions to the correlation function (1) in the perturbative limit. a) Classical diffusive propagation of a particle-hole pair in real space (left panel), and the corresponding impurity diagram in momentum space (right panel), which does not retain memory of the initial momentum and contributes to the isotropic background, Eq. (3). b) Leading contribution to the forward correlation (4). A particle-hole pair amplitude splits up into two diffusive loops traversed in opposite order (left panel). The ensuing quantum interference contribution to the correlation function (right panel) does not rely on T-invariance and is strongly peaked in forward direction, $q = 0$.

in the fermion-fermion sector. The correlation function (4) preserves the initial transverse momentum, $\mathbf{q}^\perp = \mathbf{0}$, and is sensitive to the longitudinal momentum difference $q = k_i^x - k_f^x$.

Finally, the functional average in (3) is defined as $\langle \dots \rangle_{S_0} = \int \mathcal{D}Q e^{S_0[Q]}(\dots)$, where S_0 is the celebrated diffusive σ -model action

$$S_0[Q] = \pi\nu S \int dx \text{str} \left(i\eta Q \Lambda + \frac{D}{4} (\partial_x Q)^2 \right), \quad (5)$$

where $\Lambda = \{s \delta_{ss'}\}$ is the identity matrix in boson-fermion space but breaks symmetry in advanced-retarded space. Throughout it will be convenient to think of the coordinate x in terms of some fictitious ‘time’ and of Q as a multi-dimensional quantum particle. Eq. (5) then acquires the status of a Feynman path integral, with ‘kinetic’ energy $\sim (\partial_x Q)^2$, and a ‘potential’ $\sim \eta Q \Lambda$. The latter is invariant under similarity transformations of Q leaving the diagonal matrix Λ invariant. As with a ‘radial’ potential in quantum mechanics, this high degree of symmetry will reduce the effective dimensionality of the problem and make non-perturbative calculations possible. Furthering upon this analogy, much of our analysis will rest upon a mapping of the path integral to a Schrödinger equation, which can be addressed in analogy to the quantum mechanics of centro-symmetric potentials. However, before turning to this discussion, we address the short time, or ‘strong potential’ limit, where η is large enough to confine the particle close to the origin and a formulation in terms of ‘cartesian’ coordinates is appropriate.

Diffusive short time limit $\tau \ll t \ll t_H$:—The dynamics on (real) time scales shorter than the Heisenberg time, or $\eta \gg \Delta_\xi$, can be addressed in terms of perturbation theory around the high-frequency saddle point $Q = \Lambda$ as $Q = T\Lambda T^{-1} \simeq \Lambda(1 - 2W + 2W^2 - \dots)$, where $T = \exp(W)$ and W are fluctuation generators. Individual terms in the ensuing perturbation series afford an interpretation in terms of the diffusive ‘ladder diagrams’ [6] shown in Fig. 1. The leading $\mathcal{O}(W^2)$, or zero loop order [Fig. 1, a)], contributes to the isotropic part, \mathcal{C}_0 , where it describes momentum relaxation at time scales larger than the scattering time τ . The first contribution to the forward peak arises at $\mathcal{O}(W^4)$, or two-loop order [Fig. 1 b)], as $\mathcal{C}_1(t) \propto \sqrt{t/t_H}$. This increase is fast in comparison to the $2d$ scaling $\sim t/t_H$ obtained in Ref. [3] (for a time reversal invariant setting [13]), and reflects the relatively higher phase volume accessible to diffusive fluctuations in low dimensions. The appearance of t_H as a reference scale indicates that localization is relevant to the phenomenon.

Mapping to differential equations:— For larger time scales $t \sim t_H$, or ‘weak potential’ $\eta \sim \Delta_\xi$, it is advantageous to switch from the path integral (2) to an equivalent ‘Schrödinger equation’. Its Hamilton operator,

$$\hat{H}_0 = - \left(\partial_\lambda \frac{1 - \lambda^2}{\lambda_-^2} \partial_\lambda + \partial_{\lambda_1} \frac{\lambda_1^2 - 1}{\lambda_-^2} \partial_{\lambda_1} \right) - \frac{i}{2} \eta t_H \lambda_-, \quad (6)$$

couple to the two ‘radial’ coordinates, λ, λ_1 of the quantum particle [6, 7] through a kinetic energy and a potential term, resp., where $\lambda_- = \lambda_1 - \lambda$. Central to our problem are the ground state wave function, $\hat{H}_0 \Psi_0 = 0$, $\Psi_0 = \Psi_0(\lambda, \lambda_1)$, with boundary condition $\Psi_0(1, 1) = 1$, and a perturbed wave function obeying

$$\left(2\hat{H}_0 - iq\xi \right) \Psi_1^q = \lambda_- \Psi_0, \quad (7)$$

where q is the longitudinal momentum difference. Applying the formalism of Refs. [6, 7] the main observable of interest, Eq. (4), can then be expressed as

$$\mathcal{C}_1(q, \eta) = \xi \int \frac{d\bar{\lambda}}{\lambda_-} \left[\Psi_1^q(\bar{\lambda}) + \Psi_1^{-q}(\bar{\lambda}) \right] \Psi_0(\bar{\lambda}), \quad (8)$$

where $\int d\bar{\lambda} = \int_1^\infty d\lambda_1 \int_{-1}^1 d\lambda$. The isotropic contribution \mathcal{C}_0 can be described similarly, but its explicit representation will not be needed here [12]. The behavior of the ‘wave functions’ entering (8) depends on whether we are (i) in the regime of short times $t \ll t_H$, (ii) the diffusion-to-localization crossover regime of intermediate times $t \simeq t_H$, or (iii) at asymptotically long times $t \gg t_H$. In (i), straightforward perturbation theory in weak perturbations off the configuration $\lambda = \lambda_1 = 1$ pinned by the strong potential $\eta \gg 1/t_H$ recovers the results summarized above [12]. We now proceed to explore how the

short time asymptotic connects to the perturbatively inaccessible crossover regime, (ii).

Diffusion-to-localization crossover:— At intermediate times, the primary goal is a description of the temporal buildup of the forward peak $\mathcal{C}_{\text{fs}}(t) = \mathcal{C}_1(0, t)$. Building on recent progress by Skvortsov and Ostrovsky (SO) [8] we will find that the problem possesses a surprisingly simple solution. The key observation of SO was that upon introduction of elliptic coordinates, $\lambda = \frac{1}{2}(r - r_1)$, $\lambda_1 = \frac{1}{2}(r + r_1)$, $r = \sqrt{z^2 + \rho^2}$, and $r_1 = \sqrt{(z - 2)^2 + \rho^2}$, \hat{H}_0 assumes a form similar to that of a non-relativistic $3d$ Coulomb Hamiltonian,

$$\hat{H}_0 = -\frac{r_1^2 r}{2} \left[\Delta_0 - \frac{2\kappa}{r} \right] \frac{1}{r_1}, \quad (9)$$

where $\Delta_0 \equiv \partial_z^2 + \frac{1}{\rho} \partial_\rho \rho \partial_\rho$ is the Laplace operator in cylinder coordinates (ρ, φ, z) acting in the space of azimuthally symmetric functions, and $\kappa \equiv -i\eta t_H/2$. Following Ref. [8], we can derive the ground state wave function from the known zero energy Green’s function of the $3d$ Coulomb-problem [14],

$$\left[\Delta_0 - \frac{2\kappa}{r} \right] G_0(\mathbf{r}, \mathbf{r}') = \delta(\mathbf{r} - \mathbf{r}'), \quad (10)$$

where $\mathbf{r}' = (0, \varphi, 2)$ corresponds to the boundary point $(\lambda, \lambda_1) = (1, 1) \leftrightarrow (r, r_1) = (2, 0)$. From this function, we obtain a solution to the ground state problem as, $\Psi_0(r, r_1) = -4\pi r_1 G_0(\mathbf{r}, \mathbf{r}')$, where the role of the \mathbf{r}' -inhomogeneity in (10) is to implement the boundary condition $\Psi_0(0, 2) = 1$. A solution for the Green function in terms of Bessel functions has been obtained long ago [15] as

$$G_0(\mathbf{r}, \mathbf{r}') = \frac{(\partial_u - \partial_v) \sqrt{u} K_1(2\sqrt{\kappa u}) \sqrt{v} I_1(2\sqrt{\kappa v})}{2\pi |\mathbf{r} - \mathbf{r}'|}, \quad (11)$$

where $u = r + r' + |\mathbf{r} - \mathbf{r}'|$ and $v = r + r' - |\mathbf{r} - \mathbf{r}'|$. Thanks to the appearance of the Green function, the solution to our full problem can now be formulated by standard methods of quantum mechanics. Specifically, we observe that the solution for the excited wave function (7) is obtained by convolution of the Green function (11) and the source term $\frac{1}{rr_1} \Psi_0(r, r_1)$ over the three dimensional volume element $d^3r = (rr_1/2) dr dr_1 d\varphi$. Substitution of this result into Eq. (8) then yields

$$\mathcal{C}_{\text{fs}}(\eta) = 32\pi \xi \langle \mathbf{r}_0 | \hat{G}_0 \frac{1}{\hat{r}} \hat{G}_0 \frac{1}{\hat{r}} \hat{G}_0 | \mathbf{r}_0 \rangle \stackrel{(10)}{=} 8\pi \xi \partial_\kappa^2 G_0(\mathbf{r}_0, \mathbf{r}_0).$$

To compute the κ -derivative, we regularize the Green function in (11) as $G_0(\mathbf{r}_0, \mathbf{r}_0) = \lim_{\mathbf{r} \rightarrow \mathbf{r}_0} G_0(\mathbf{r}, \mathbf{r}_0)$. A straightforward Taylor expansion of Bessel functions then leads to

$$\mathcal{C}_{\text{fs}}(\eta) = 8\xi \partial_\kappa K_0(4\sqrt{\kappa}) I_0(4\sqrt{\kappa}) \Big|_{\kappa = -i\eta \frac{t_H}{2}}. \quad (12)$$

Upon Fourier transformation, the time dependence of the forward-scattering peak contrast is finally obtained as (cf. Fig. 2)

$$\frac{C_{\text{fs}}(t)}{C_{\infty}} = \theta(t) I_0 \left(\frac{2t_H}{t} \right) e^{-2t_H/t}, \quad (13)$$

where $C_{\infty} = C_{\text{fs}}(\infty)$ is the long term asymptotic to be discussed momentarily. The limiting behavior of I_0 [16] implies the long and short time expansions

$$\frac{C_{\text{fs}}(t)}{C_{\infty}} = \begin{cases} \frac{1}{\sqrt{2\pi}} \left(\left(\frac{t}{2t_H} \right)^{\frac{1}{2}} + \frac{1}{8} \left(\frac{t}{2t_H} \right)^{3/2} + \dots \right), & t \ll t_H, \\ 1 - 2\frac{t_H}{t} + 3 \left(\frac{t_H}{t} \right)^2 + \dots, & t \gg t_H, \end{cases}$$

generalizing the previously studied limit.

Long time limit $t/t_H \gg 1$ and saturation value of contrast:—For $\eta \ll t_H^{-1}$, fluctuations far away from the origin $(\lambda, \lambda_1) = (1, 1)$ become energetically affordable. In this regime, dominant contributions to correlation functions come from the integration over $\lambda_1 \gg \lambda \sim 1$. To leading approximation the dependence of the differential equations on λ may be ignored [6, 7], and the solution for the dependence on the ‘non-compact’ variable λ_1 along the lines of [6] obtains

$$C_1(q, \eta) = \frac{8i\xi}{\eta t_H} \text{Re} \int_0^{\infty} dx \int_0^x dy x K_1(x) K_{\sigma_q}(x) y K_1(y) I_{\sigma_q}(y),$$

where $\sigma_q = \sqrt{1 - 4iq\xi}$, and K_{ν} and I_{ν} are the modified Bessel functions of order ν . The $\sim \eta^{-1}$ -scaling of this result implies a trivial (constant) time dependence $C_1(q, t) \equiv C_{\infty}(q)$ at large times, where the saturation function, $C_{\infty}(q)$, is determined by the coordinate integrals. The isotropic component, C_0 , turns out to be given by the same expression, at, however, $q = 0$. In other words, the forward scattering amplitude and the isotropic component coincide at large times, $C_{\text{fs}}(t = \infty) = C_0(t = \infty) \equiv C_{\infty}$, which means that the forward scattering peak asymptotes to a value twice as large as the isotropic background. The saturation value $C_{\infty}(q)$ as a function of longitudinal momentum difference is shown in the left inset of Fig. 2. The amplitude rapidly decreases as a function of q , half of the peak value C_{∞} is reached at the characteristic scale $q \simeq \xi^{-1}$, and for larger values the peak amplitude decays as $\sim q^{-2}$. Since the localization length is much larger than the mean-free path l , this narrow peak should be easily distinguished from the broadened energy shell in k -space.

So far, we have assumed an initial state of sharply defined momentum. To account for the presence of momentum spread we convolute our results over a distribution of initial momenta. For a Lorentzian distribution of width Δk , we find $\langle C_{\text{fs}}(\infty) \rangle = C_1(i\Delta k, \infty) = C_{\infty}(i\Delta k)$, where C_{∞} is the peak function discussed above. The forward signal, shown in the left inset of Fig. 2, will be severely

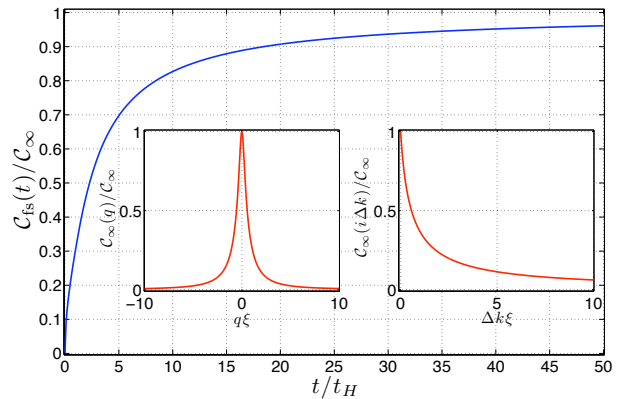


FIG. 2: Forward-scattering peak contrast, Eq. (13), as a function of time t/t_H . Insets: Saturation value as a function of longitudinal momentum difference q (left) and spread Δk of the initial state (right).

suppressed once $\Delta k > \xi^{-1}$. Qualitatively similar behavior is expected for other distributions, which means that near monochromatic initial configurations are vital for the observability of the forward peak.

Discussion:—Previous experiments [4, 5] have probed the coherent response of atomic clouds to a speckle potential quench to two-dimensional disorder. In these systems, a crossover to effectively *three*-dimensional dynamics (with only very weakly developed signatures of quantum interference) occurred at rather short times $t \ll t_H$, which means that a coherent backscattering peak, but no forward peak could be observed. With this paper, we propose to repeat the quench experiment in a quasi one-dimensional setting with its parametrically shorter Heisenberg time, and stronger developed localization which will cause a more rapid increase of the forward signal. The quasi one-dimensional geometry is realized if $L_{y,z} \ll \xi \ll L_x$, where the localization length ξ is of the order Nl , and N is the number of channels introduced by transverse size quantization.

For this type of system, our theory predicts the power law increase of a forward signal at short times, the saturation dynamics at large times, the momentum dependence of the forward signal, and its dependence on the width of the initial state. In total, this is the first space/time resolved portrait of a strong localization phenomenon, with the perspective of observation using current experimental technology of cold atom physics or photonics [17].

T. M. would like to thank M. Micklitz for fruitful discussions. Work supported by FAPERJ (Temático and Infra 2013) and SFB/TR 12 of the Deutsche Forschungsgemeinschaft.

[1] Strong localization in a driven chaotic system has been observed by J. Chabé, *et al.*, Phys. Rev. Lett. **101**,

- 255702 (2008). Localization of cold atoms in strictly one-dimensional wave guides has been seen in J. Billy *et al.*, Nature **453**, 891 (2008) and G. Roati *et al.*, Nature **453**, 895 (2008).
- [2] N. Cherroret, T. Karpiuk, C. A. Müller, B. Grémaud, and C. Miniatura, Phys. Rev. A **85**, 011604(R) (2012).
- [3] T. Karpiuk, N. Cherroret, K. L. Lee, B. Grémaud, C. A. Müller, and C. Miniatura, Phys. Rev. Lett. **109**, 190601 (2012).
- [4] F. Jendrzejewski, K. Müller, J. Richard, A. Date, T. Plisson, P. Bouyer, A. Aspect, V. Josse, Phys. Rev. Lett. **109**, 195302 (2012).
- [5] G. Laberie, T. Karpiuk, J.-F. Schaff, B. Grémaud, C. Miniatura, D. Delande, Eur. Phys. Lett. **100**, 66001 (2012).
- [6] K. B. Efetov, *Supersymmetry in Disorder and Chaos* (Cambridge U. Press, 1999).
- [7] K. B. Efetov and A. Larkin, Sov. Phys. JETP **58**, 444 (1983).
- [8] M. A. Skvortsov and P. M. Ostrovsky, JETP Lett. **85**, 72 (2007).
- [9] J. Dalibard, F. Gerbier, G. Juzeliunas, P. Öhberg, Rev. Mod. Phys. **83**, 1523 (2011).
- [10] T is already broken by fields of classically vanishing strength with a few flux quanta through the area $\mathcal{O}(L_{\perp}\xi)$, where ξ is the localization length and L_{\perp} the transverse width.
- [11] T. Plisson, T. Bourdel, C. A. Müller, Eur. J. Phys. ST **217**, 79 (2013).
- [12] Further details will be published elsewhere.
- [13] The crossing diffusons should also be included in the time-reversal symmetric case of Ref. [3]. At two-loop order, they yield the same forward correlation as the concatenated maximally-crossed diagrams.
- [14] J. Meixner, Math. Z. **36**, 677 (1933).
- [15] L. Hostler, Bull. Am. Phys. Soc. **7**, 609 (1962); L. Hostler and R. H. Pratt, Phys. Rev. Lett. **10**, 469 (1963).
- [16] I. S. Gradshteyn and I. M. Ryzhik, *Table of integrals, series, and products* (Academic Press, New York, 2000).
- [17] T. Schwartz, G. Bartal, S. Fishman, and M. Segev, Nature **446**, 52 (2007).